


Volker Bächle*
Marco Gleiß
Hermann Nirschl

Influence of Particles on the Roller Discharge of Thin-Film Filtration without Gas Throughput

If fine and compressible particle systems need to be separated, the ground layer compaction caused by the compacting of the filter cake leads to high flow resistances. Thin-film filtration is a suitable method to avoid the limiting effect of the filter cakes. Gas-impermeable filter membranes prevent shrinkage cracking, which can occur during demisting of the filter cakes. Titanium dioxide and baker's yeast are used as model particle systems, which are present in different concentrations and are filtered with track-etched membranes in different particle-to-pore size ratios. The parameters determined during the investigation are the residual moisture, the specific solid mass, and the completeness of the discharge. Filtration causes progressive blocking of the membrane pores, resulting in filter medium resistances that are increased by up to a factor of 175. Metabolism of yeast can cause bubbles to accumulate on the membrane and decreasing the free filter area. Without regeneration the specific solid mass flow rate is reduced by 61 % for titanium dioxide and by 13 % for yeast under ideal conditions of this experimental study.

 This is an open access article under the terms of the Creative Commons Attribution License, which permits use, distribution and reproduction in any medium, provided the original work is properly cited.

Keywords: Drum filter, Membranes, Roller discharge, Solid mass flow rate, Thin-film filtration

Received: May 19, 2023; *revised:* July 23, 2023; *accepted:* August 31, 2023

DOI: 10.1002/ceat.202300249



Supporting Information
available online


1 Introduction

The separation of disperse particles from a continuous liquid phase is one of the fundamental basic operations of mechanical process engineering. Separation tasks can be found in almost every branch of industry and influence both daily life and our environment through their separation success and separation efficiency [1]. For sustainable handling of chemical raw materials, minerals, and ores or biological substances, it is important to carry out separation processes as efficiently as possible and in a way that conserves resources [2, 3]. A reduction in the required energy with increasing separation success thus holds great potential for optimization. For example, according to Molina Grima et al., the separation of biomass from liquid in microalgae amounts to 20–30 % of the total costs [4]. These difficult to filter particles like microalgae, yeast or titanium dioxide (TiO₂) are still a challenge regarding the harvesting or extraction.

A usual separation via centrifuge produces reliable and good results. However, especially with biological products, the density difference between particles and liquid is low, which is why high accelerations are required. According to Hermeler et al., 50 % of the energy input is due to the acceleration of the liquid [5]. Other methods are flocculation and precoat filtration, both of which use additives (flucclants, cellulose) and thus contaminate

the value product [6–9]. Cross-flow filtration can be used to filter such particles, but they are only concentrated [10–14]. Rios et al. achieved an increase in the concentration of *Nannochloropsis salina* from 0.095 to 8 g L⁻¹ [15]. However, further concentration requires a recoverable retentate [16]. High cake resistances due to compressible behavior also rule out the filter press, which requires high filtration times due to the high cake resistances [17–19].

One possibility for filtering these particles is thin-layer filtration using a drum filter. The drum filter has the integration of several process steps in one unit. In this way, cake formation, demisting, and discharge can take place within one rotation cycle of the rotary filter. The high degree of flexibility of the apparatus, in combination with fully continuous operation, leads to high performance. While the horizontal drum, which is immersed in a suspension trough, rotates, the filtrate flows into the interior due to the vacuum. A filter cake forms on the

Volker Bächle  <https://orcid.org/0000-0001-8708-3408>
(volker.baechle@kit.edu), Dr.-Ing. Marco Gleiß,
Prof. Dr.-Ing. Hermann Nirschl
Karlsruhe Institute of Technology (KIT), Institute of Mechanical
Process Engineering and Mechanics (MVM), Strasse am Forum 8,
76131 Karlsruhe, Germany.

outside of the drum, which is covered with filter media, and is removed from the apparatus during the rotation cycle. Currently, mainly conventional filter cloths are used as cost-effective filter media for covering cake-forming rotary drum filters. However, due to their mostly woven structure, cake cracking occurs in the case of compressible particle systems, resulting in leakages that allow gas to enter the interior of the drum [1, 20]. A leakage of gas also causes a drop in pressure inside the cake, which means that the remaining pores can no longer be demoistured.

Semipermeable membranes prevent transmembrane gas flow due to small pore sizes and high capillary inlet pressures, shown in Fig. 1. The capillary inlet pressure is defined according to Eq. (6) (see Sect. 2.3). If the actual pore size is smaller than this equivalent diameter of the capillary pressure, the gas cannot penetrate the completely moistened hydrophilic pores. In contrast, with larger pores, the gas differential pressure pushes the pores free and gas penetrates into the filtrate. However, their lower mechanical stability limits the application areas of filter membranes.

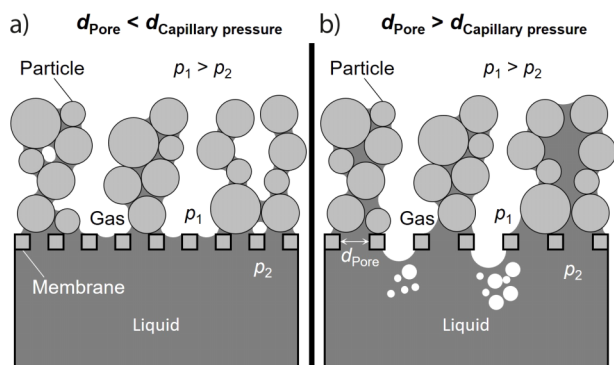


Figure 1. Schematic illustration of the dehumidification behavior of a filter cake in filtration without gas throughput (a) and filtration with leakage through pores with a diameter larger than the equivalent capillary diameter (b).

Rubberized rollers detach filter cakes from filter media surfaces at lower mechanical forces and can thus be used on vacuum drum filters [21]. The pore sizes of filter membranes are related to the particle separation mechanisms of a surface filtration, which significantly influences the cake formation [22]. Compressible particle systems in particular form very thin but porous cakes during filtration, which can be detached from the membrane with varying efficiency depending on the drum and roller speed, roller contact pressure, and direction of removal [21]. The formation of thin filter cakes is utilized in thin-film filtration, since the flow resistance of the cake rises with increasing cake height. In order to prevent the resulting decrease in filtration performance, filter cakes are removed before large losses in performance become noticeable [23].

Previous investigations indicate that complete cake removal is possible with rubberized rollers with different differential pressures and that roller rotation has only a minor effect on a membrane without prior filtration [24]. However, the influence of particles on roller discharge is only slightly considered. Therefore, this paper aims to investigate the influence of the

particle system on roller discharge based on the studies by Lam et al. [21, 24]. It is to be examined to which extent the solid material has an effect on the acceptance quality. A comparison between the inorganic white pigment TiO_2 and the biological model organism yeast enables the influence of the material on the roller discharge of pasty filter cakes to be investigated.

The quality of the removal properties of the filter cakes on a laboratory drum filter are recorded by means of the residual moisture, area-specific solid mass, and completeness of the discharge. Five different track-etched membranes with nominal pore sizes between 0.2 and $3.0 \mu\text{m}$ are used to assess the filter properties with varying particle-pore size ratios. The fouling behaviour of the filter media and its effect on the removable solids mass, cake residual moisture, completeness of discharge, and membrane resistance are also checked.

2 Materials and Methods

2.1 Sample Preparation and Characterization

The first model particle system is TiO_2 from Venator Germany GmbH (Duisburg, Germany) with an average particle size of $\bar{x}_{50,3,\text{TiO}_2} = 0.55 \mu\text{m}$. The particle size is determined by laser diffraction spectroscopy on an LBS Helos Quixel from Sympatec GmbH (Basel, Switzerland). For representative results, the particles of a single charge (Hombitan[®]; LO-CR-S-M; D9Q008/83) are used. For the experiments, the TiO_2 is suspended in distilled water with 5 wt % mass concentration and reaches a pH of 9.6 after suspension, measured at a temperature of 20°C (WTW pH 3310, Xylem Analytics Germany GmbH, Weilheim, Germany). The cake resistance R_C is determined to $4 \times 10^{15} \text{m}^{-2}$ with a pressure nutsche according to VDI guideline 2762-2 at 0.8 bar. Analogously, the filter medium resistance is defined as R_{FM} .

The second particle system is the commercial baker's yeast *Saccharomyces cerevisiae* from FALA GmbH (Kehl, Germany) with a mean particle diameter of $\bar{x}_{50,3,\text{Yeast}} = 4.2 \mu\text{m}$. The yeast is available in pressed form as fresh yeast and has a bio-dry matter content of 32 wt %. For the experiments, the yeast is suspended in deionized water with 2 wt % bio-dry mass. In addition to the yeast cells, 0.9 wt % sodium chloride is added to the continuous phase deionized water [25]. The pH is 4.1 after suspension from 18°C . For experiments with increased cell metabolism, another 10 wt % of fresh yeast mass of sugar is added to the suspension. The dry mass is determined for both particle systems after a storage time of 24 h in an oven at 95°C . The cake resistance is $2.7 \times 10^{14} \text{m}^{-2}$ with 0.8 bar differential pressure. The mass concentration selected is 5 wt % for TiO_2 and 2 wt % yeast, as these produce cake heights of 1 mm with a new membrane under the conditions mentioned in Sect. 2.3. Cakes with 1 mm height are considered thin layers, which is why this is defined as the initial cake level [24].

2.2 Filter Medium

For the experiments, five track-etched membranes with pore diameters between 0.2 and 3.0 μm are used (RoTrac[®] from Oxyphen GmbH, Lottstetten, Germany; TrakEtch[®] from SABEU GmbH & Co. KG, Northeim, Germany). The membranes used have a supporting structure to take up mechanical forces. Track-etched membranes have a very small pore size distribution, which is advantageous for the analysis of the pore-to-particle ratio. The polyethylene terephthalate (PET) material exhibits good resistance to abrasion, which is needed for roller discharge. Tab. 1 shows the relevant material data of the membranes.

2.3 Experimental Setup and Procedure

For an investigation of the cake removal behavior on a vacuum drum filter, this is equipped with a track-etched membrane. As shown in Fig. 2, the drum filter is equipped with a roller discharge, which is pressed onto the membrane via two springs. The operating parameters are chosen from the results of Lam et al. and include a pressureless cake removal with a line pressure force q_p of 444.2 N m^{-2} . The line pressure force is defined as the linear pressure with which the roller presses on the membrane and is defined according to Eq. (1) [24].

$$q_p = \frac{2 Ds}{L} \quad (1)$$

Here, D describes the spring rate, s the spring travel, and L the roller length. The roller, rubberized with acrylonitrile butadiene rubber, has a diameter of 60 mm, a Shore A hardness of 34°, and a length of 200 mm. The removal roller rotates at the same circumferential speed as the drum with an adjustable direction of rotation. A distinction is made between the same and opposite directions of rotation. With the same direction of rotation, the speed vector at the contact surface of roller and drum points in the same direction, vice versa for the opposite direction. With these settings, a shear force of 11.36 N results for the opposite direction discharge. The shear force is deter-

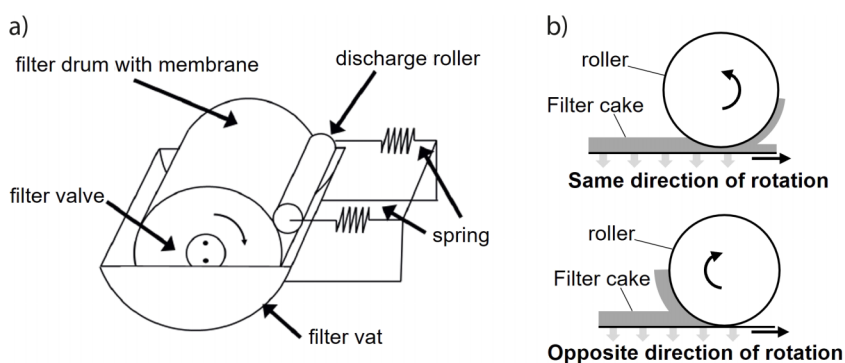


Figure 2. Vacuum drum filter in use with roller discharge (a) and schematic diagrams of the discharge direction (b) [24].

mined from the difference in power consumption between no-load and contact stress of the motor (MFA – Como drills, 919D Series). With the efficiency of the motor and the rotation speed of the roller, the torque and thus the shear force on the membrane can be calculated.

The drum of the drum filter has a diameter of 300 mm and is immersed in the suspension up to a cake formation angle of 90°. The cake formation angle results in a cake formation time of 11.3 s with a subsequent demoinsture time of 16.9 s. The total cycle time is 45.2 s, leading to a circumferential speed of 0.021 m s^{-1} for the drum. This circumferential speed is identical to the roller, which results in a higher rotational speed with a smaller diameter.

With the aid of the drum filter, the membranes are examined for their interaction with the particle system during roller discharge. For this purpose, the membranes are attached to the drum filter and the aforementioned suspensions are filtered. After cake discharge with the roller, the cake is manually discharged from the roller with a spatula. After every 5-th rotation, the cake is gravimetrically determined and then dried in a drying oven at 95 °C for 24 h. The cake is removed from the roller with a spatula. Based on the mass difference of solid M_S and evaporated liquid M_L , the residual moisture of the filter cake can be determined according to:

$$RM = \frac{M_L}{M_{\text{Cake}}} \times 100 \% = \frac{M_L}{M_L + M_S} \times 100 \% \quad (2)$$

Table 1. Overview of the track-etched membranes used with ^{a)}manufacturer's specification and ^{b)}measurement on the porometer.

| Membrane specification and material | Pore size ^{b)} [μm] | Pore density ^{a)} [10^6 cm^{-2}] | Air flow rate ^{a)} [$\text{min}^{-1} \text{ cm}^{-2} \text{ bar}^{-1}$] | Total thickness ^{a)} [μm] |
|-------------------------------------|---|---|--|---|
| TrakEtch [®] 0.2 (PET/PET) | 0.22 ± 0.01 | 320 ± 50 | 4.2 ± 0.7 | 150 ± 30 |
| RoTrac [®] 0.4 (PET/PP) | 0.40 ± 0.04 | 100 ± 15 | 8.0 ± 4.0 | 170 ± 50 |
| RoTrac [®] 0.8 (PET/PET) | 0.80 ± 0.08 | 50 ± 7 | 17.0 ± 4.0 | 150 ± 50 |
| TrakEtch [®] 1.0 (PET/PP) | 0.97 ± 0.03 | 23 ± 3 | 23.8 ± 3.0 | 170 ± 50 |
| RoTrac [®] 3.0 (PET/PET) | 3.00 ± 0.30 | 2.0 ± 0.3 | 30.0 ± 9.0 | 150 ± 50 |

Furthermore, the removed mass must be characterized. Both the removed cake and the residue remaining on the membrane are weighed separately, so that a residual cake moisture (according to Eq. (2)), the absolute discharge mass, and the completeness of the discharge Q according to Eq. (3) can be quantified. Analogous to the determination of residual moisture, a thermal post-demoisturing of the samples in the drying oven is necessary.

$$Q = \frac{M_{S,Cake}}{M_{S,Cake} + M_{S,Residue}} \times 100 \% \quad (3)$$

In general, the specific solid mass flow \dot{m}_s at a drum filter can be defined according to Eq. (4) [1]. This is the general equation for determining the mass flow on a drum filter and shows the dependence of the individual parameters on the solids mass flow.

$$\dot{m}_s = \frac{\dot{M}_s}{A_{Filter}} = (1 - \varepsilon) \times \rho_{Particle} \times \sqrt{\frac{2P_{Cake}}{\eta_L}} \times \sqrt{\kappa \Delta p n} \times \sqrt{\frac{\alpha_{Formation}}{360^\circ}} \quad (4)$$

In this paper, the filter cake was removed cyclically, which is why the removed solids mass is defined via m_{sc} in Eq. (5). m_{sc} is measured gravimetrically here. Here t_{cycle} is the time of cake formation per cycle, which is 11.3 s. Thus, it is possible to calculate back to the solid mass flow.

$$m_{sc} = \frac{\dot{m}_s}{t_{cycle}} \quad (5)$$

Experiments to determine the pore size and its distribution are carried out on a capillary flow porometer (CFP-1500AEX; Porous Materials Inc; Ithaca, USA). For this purpose, samples with a diameter of 22 mm are used with silicone oil AK 10TM from Wacker Chemie AG with a surface tension of $\gamma = 20 \text{ mN m}^{-1}$ and the contact angle is assumed to be $\Theta = 0^\circ$ due to complete moistening. The equation to determine the pore size is Eq. (6) with P_{cap} as the capillary pressure [1].

$$d_{capillary\ pressure} = \frac{4\gamma_L \cos \theta}{P_{cap}} \quad (6)$$

For resistance measurements of membrane and filter cake, a pressure nutsche according to VDI 2762-2 is available, which is

operated with a pressure difference of 0.8 bar. The filter media area is 19.64 cm^2 and the resistances of the cake R_C and filter media R_{FM} can be calculated via Eq. (7):

$$\frac{t_{cycle}}{V_{F,cycle}} = R_C \times \frac{\eta_L \kappa}{2A_{Filter} \Delta p} \times V_{F,cycle} + R_{FM} \times \frac{\eta_L}{A_{Filter} \Delta p} \quad (7)$$

Here, $V_{F,cycle}$ is the filtrate volume, which can be calculated into a mass via the density of the fluid water. If the quotient of time t_{cycle} and $V_{F,cycle}$ is plotted over $V_{F,cycle}$ during filtration, a straight line is obtained. From this straight line, the cake resistance R_C can be determined via the slope and the filter media resistance R_{FM} via the initial value of the filtration ($V_{F,cycle} = 0$). A laser scanning microscope (VK-X100k; KEYENCE Deutschland GmbH, Germany) is available for optical examinations.

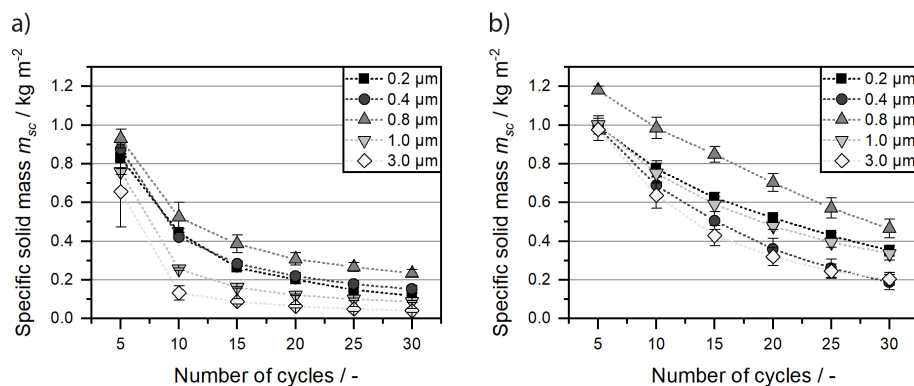
3 Results

3.1 Influence of the Pore Size and Rotational Direction

Fig. 3 visualizes the area-specific solid mass of TiO_2 for 5 wt % over the number of cycles for the entire spectrum of membrane pore sizes in both discharge directions. The specific solid mass is the effective removed solid mass per filter area. For both rolling directions, the $0.8\text{-}\mu\text{m}$ membrane shows the maximum solids mass flow, while the membrane with a nominal pore size of $3.0\text{ }\mu\text{m}$ exhibits the greatest reduction in specific solids mass flow. In the case of the opposite direction of discharge, this is coupled with the highest variance.

The decrease in the same direction in Fig. 3b shows similar curves for the two TrakEtch[®] membranes (0.2 and $1.0\text{ }\mu\text{m}$), and four membranes (0.2 , 0.4 , 1.0 , $3.0\text{ }\mu\text{m}$) demonstrate an almost identical initial value of the first reductions. A comparison of the removal directions indicates that the rotation of roller and drum in the same direction leads to higher solid mass flows. Due to the high contact pressure of the drum, particles are pressed into the pores of the membrane, which reduces the effective filter area. In addition to the passive blocking of free pores by the fluid forces caused by the flow, this active mechanism leads to increasing fouling of the membrane. This is comparable to the experiments of Tran et al. [26], who had a reduction of 80 % of the flux when filtering 1.5 L of water with natural organic matter. Without suitable regeneration and

Figure 3. Comparison of the discharged specific solid mass per cycle for titanium dioxide with 5 wt % for the opposite direction of discharge (a) and same direction of discharge (b) with a variation of the pore size.



cleaning measures, a complete loss of the separation performance of the membranes is to be expected [27, 28].

When considering the completeness of the discharge, it is valid that reaching a value of 100 % corresponds to a complete, ideal cake detachment. This means that no solid remains on the membrane, as the roller removes the entire cake. Fig. 4 shows the cake residue on the membrane after roller discharge. As can be seen in Fig. 4, a complete removal is not achieved which is due to boundary effects. Especially with cake heights of 1 mm, the cake extends beyond the membrane edge and cannot be collected by the roller.

The completeness, which can be regarded as independent of the membrane at the beginning of the filtration, decreases with increasing number of cycles. While the completeness of the counter-rotational discharge shows similar values with a higher number of filtration cycles, the proportion of the removed solid mass decreases continuously in the same rotational direction. The behaviour of the opposite direction of rotation can be described as an exponential decrease with a horizontal asymptote, since an approximately stationary final value is reached. The decrease in the removed mass can be explained by a particle film on the roller. The particle film causes the roller to lie unevenly on the drum, resulting in areas without direct contact between roller and drum. Thus, a particle film remains on the membrane in these areas. This effect is more pronounced with the 3.0- μm membrane.

The course of the 0.4- μm membrane, in the same rotational direction, is notable. The decreasing trend means that the mechanical load on the roller has a greater influence on the filtration performance of these membranes as the number of cycles rises. This makes them less suitable for thin-film filtration of TiO_2 on the drum filter. This can be attributed to the pore-to-particle ratio, which is 1.38 for a pore size of 0.4 μm and a mean particle size of 0.55 μm . Individual particles are therefore pressed into the pores during cake removal and block them. Therefore, no loose particle bridges or loosely lying particles are formed on the surface. As a result, the lowest particle layer is firmly attached to the membrane and high cohesive forces cause the cake to tear into two layers. This effect does not occur with the opposite discharge, as the particles are still sheared off the surface.

The influence of pore size on the residual moisture in the filter cake is negligible. The residual moisture is constant at 36.5 % for the opposite rotational discharge, 3 % higher than the same rotational discharge at 33.45 %. Pressing the roller onto

the cake thus reduces the residual moisture. In comparison to Lam et al. a deviating trend is displayed here. These tests were carried out without a pressure difference during discharge, which is why the residual moisture is lower in the same rotational direction. In Lam et al. this is reversed, as the cake could be further demineralized by a circulation during the opposite-direction discharge with simultaneous pressure difference [21].

Analogous to the TiO_2 results, the decreasing course of the specific solid mass for yeast with 2 wt % in Fig. 5 implies stronger fouling of the membrane with increasing number of removal cycles. Both cakes here have a cake height of 1 mm with a new membrane. The reduction is less pronounced than with TiO_2 , but shows a dependence on the choice of membrane. The membranes with a nominal pore size of 0.8 and 1.0 μm exhibit the largest reduction in mass for both rolling directions in comparison, while both the membrane with the largest and the smallest nominal pore size show decreasing curves. In the case of the small pores, this can be attributed to the extracellular polymeric substances (EPS), which can close small pores through a biofilm. These substances can occur due to stress situations such as temperature changes in organic particles.

The 0.4- μm membrane is the borderline case here, as the EPS can penetrate through the 0.8- μm membrane and thus do not block the pores. Therefore, the discharge is not as pronounced as with the smaller pore size. For the membrane with

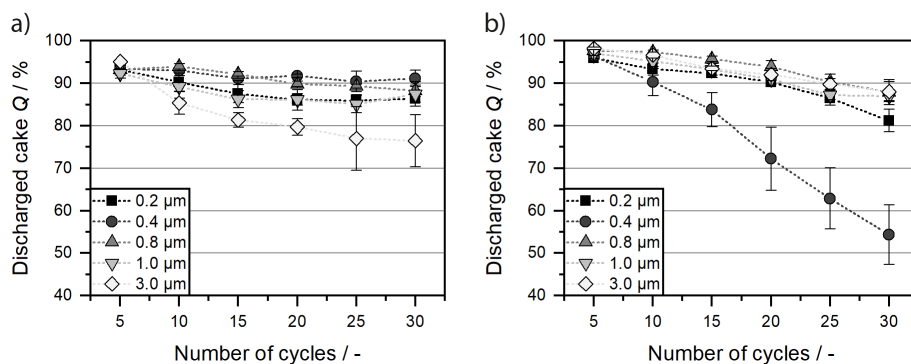


Figure 4. Comparison of the discharged cake completeness for titanium dioxide with 5 wt % for the opposite direction discharge (a) and the same rotational direction (b) with a variation of the pore size.

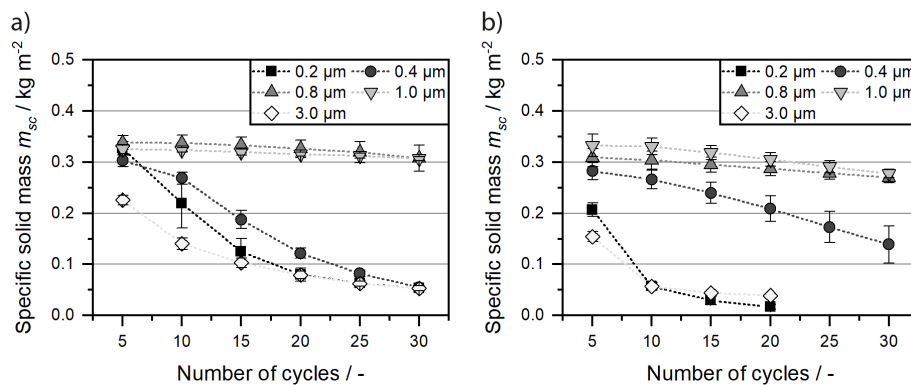


Figure 5. Comparison of the discharged specific solids mass per cycle for yeast with 2 wt % for the opposite roller discharge (a) and same rotational direction (b) with a variation of the pore size.

3.0 μm pore size and 4.2 μm mean particle size, the particle-to-pore ratio is again similar with 1.4 as for TiO_2 with 1.38 with 0.4 μm pores. Here again the effect of clogging occurs. With the membranes (0.2 μm ; 3.0 μm) there are only 20 discharge cycles, since the filter cake with <0.1 mm is completely dried to the membrane by the demisting time of 16.9 s in the ambient air and thus a discharge is no longer possible. Therefore, further tests were not carried out.

In the case of the same rotational direction, the reductions (0.4 μm ; 0.8 μm ; 1.0 μm) in Fig. 5b can be described with an exponential curve. Regardless of the direction of rotation, the solid mass flows of the 0.8- μm and 1.0- μm membranes decrease almost linearly. Within the first 30 removal cycles in opposite directions, a reduction of 9.1 % of the removal mass can be observed for the 0.8- μm membrane and a reduction of 5.6 % for the 1.0- μm membrane. In addition, it can be seen that the removal direction only has an effect on the mass flows as the number of discharge cycles increases. The fact that it is precisely these two membranes that turn out to be the most efficient pore sizes is in line with the practical recommendation for selecting the pore size for the filtration of yeasts found in [29].

A comparison of the proportionally removed solid mass in Fig. 6 only reflects the irregular behavior of the 0.2- μm and 3.0- μm membranes in the case of same rotational direction due to large deviations or a strong reduction in completeness. As described by Lam et al., the opposite-direction roller discharge enables an almost complete discharge of the cake [21]. This shows an atypical behavior, as the influence of the membrane pore size declines with increasing number of removal cycles. Here again, there is a difference in the decrease directions, since the completeness of the 0.4- μm as well as the 0.8- μm and 1.0- μm membrane is independent of the same rotational cycle number. With the use of the 3.0- μm membrane, a similar behavior is seen in the discharge completeness as before with TiO_2 , as here the particle to pore ratio is 1.4 and therefore pores get clogged. A remaining particle layer is the result, which divides the cake during discharge due to cohesive forces.

Analogous to the inorganic particle system, the uniaxial pressure load of the same rotational direction of the roller lowers the residual moisture and is independent of the pore size. The demisting consolidation is pronounced for all membrane pore sizes. For example, the residual moisture of the

0.8- μm membrane (same direction: 64.3 %; opposite direction: 68.5 %) is 4 % lower when the cake is removed using a roller rotating in the same direction.

3.2 Effects on the Membrane

For a better overview of the influence of the roller discharge with different particle-to-pore ratios, an investigation is carried out according to the discharges of the membrane under the porometer and pressure nutsche. In accordance with the thesis of permanent pore blocking by particles, the filter medium resistance R_{FM} increases due to filtration.

Tab. 2 indicates that the opposite direction of discharge leads to a stronger impairment of the membranes, which is reflected in resistances that are higher by a factor of 10–175. The absence of shear stress due to the same rotational direction results in significantly lower filter mean resistances. The increase in resistance across the pore size is also notable. This follows from lower resistances with larger pores of new membranes. After the filtrations, the absolute resistances of all membranes are in the same order of magnitude of $5 \times 10^{11} \text{ m}^{-1}$.

Table 2. Overview of the increase of filter media resistance $R_{\text{FM}}/R_{\text{FM,unused}}$ after drum filtration of yeast and TiO_2 .

| Membrane pore size [μm] | 0.2 | 0.8 | 3.0 |
|--------------------------------------|-------|-------|--------|
| Yeast – opposite direction | 19.58 | 1.28 | 1.47 |
| Yeast – same direction | 40.02 | 0.76 | 1.50 |
| TiO_2 – opposite direction | 22.10 | 88.95 | 175.06 |
| TiO_2 – same direction | 4.97 | 16.55 | 4.56 |

With the filtration of yeast, no significant decrease in pore size is visible with the porometer, but under the pressure nutsche the filter resistance increases up to a factor of 40. This indicates a film on the surface of the membrane, which covers part of the filter area and at the same time no entry into the pores, which reduces them. The absolute pore sizes of the membranes are given in Tab. 3.

With yeast, there is no increase in the mean pore size for the 0.2- μm and 0.8- μm membrane, which indicates pure deposition on the surface. Only the 3.0- μm membrane decreased to 1 μm , which reflects the interaction with the particles. The direction of discharge is irrelevant. With TiO_2 , the pore size decreases to 0.127 μm on average for all membranes and used discharge directions. Only with the 3.0- μm membrane can the separation of the particles by the cohesive forces during the same rotational direction discharge be clearly detected. Images of the membrane surface with a laser-scanning microscope can be found in the Supporting Information.

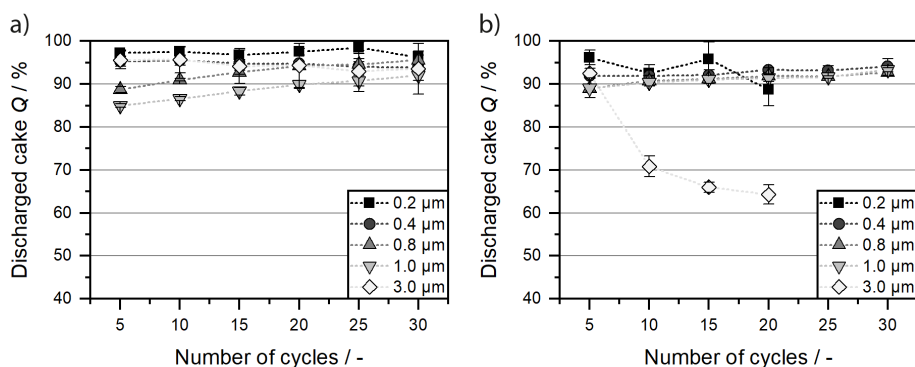


Figure 6. Comparison of the discharged cake for yeast with 2 wt% for the opposite roller discharge (a) and same rotational direction (b) with a variation of the pore size.

Table 3. Overview of the mean flow pore diameters after drum filtration of yeast and TiO₂.

| Membrane pore size [μm] | 0.2 | 0.8 | 3.0 |
|---------------------------------------|-------|-------|-------|
| Yeast – opposite direction | 0.191 | 0.719 | 1.072 |
| Yeast – same direction | 0.176 | 0.775 | 1.012 |
| TiO ₂ – opposite direction | 0.124 | 0.130 | 0.123 |
| TiO ₂ – same direction | 0.126 | 0.133 | 0.435 |

Furthermore, an investigation was done regarding the filtration behavior with fresh and frozen cells and filtration with additional metabolism of yeast, which is also presented in the Supporting Information.

4 Conclusion

The investigations for both particle systems, TiO₂ and yeast, showed that the interaction between membrane, particle, and roller does have an effect on roller discharge and the associated fouling. The decreasing course of the removed mass takes place under all filtration conditions for both particle systems and is due to the progressive blocking of pores, the membrane fouling. Microscopically, particles block free pore channels and deposit in the area of the pore mouths or in the pore capillaries. Solid adsorption reduces the effective filter area, resulting in a decrease in filtration performance in the form of decreasing removal masses. This relationship is confirmed by the increased filter media resistances and decreasing mean flow pores of the filter membranes after drum filtration.

As the number of cycles increases, the track-etched membranes are subjected to mechanical stress. This results in the overlapping of pressure and shear forces in the opposite direction of rotation, which lead to the break-up of the cake structure and push particles deeper into the filter pores or shear off pressed-in particles from the cake. Accordingly, the solid mass decreases significantly more with the opposite direction of rotation as the number of cycles increases. With regard to the filter medium resistances and pore size, the opposite direction of rotation can be classified as disadvantageous, since higher resistances and lower values of the mean flow pores result from the filtration.

Metabolism, growth, and multiplication of organic cell cultures are strongly temperature-dependent. Tempering of the yeast suspension shows that metabolism influences the filtration properties by increasing cake porosity. This is due to the pore-blocking effect of CO₂ and extracellular polymeric substances. If metabolism is stopped or terminated, the specific solid masses show a slightly increasing trend with the increase in temperature. In general, however, metabolism is to be classified as disadvantageous to roller discharge and should be avoided.

With frost-treated yeast, filter cakes with 8 % lower residual moisture content can be removed. However, if the yeast is fresh, the specific solids mass is 2–3 times greater in the first 30 cycles without intermediate membrane regeneration. The thermal conditioning of the cells has a significant influence on the

filtration properties. The background for this is also the reduction of the effective bio-dry mass content, since yeast cells show a lower bioactivity after storage below the freezing point.

The results of this paper can be summarized as follows:

- Due to the particle interaction with the membrane, continuous roller discharge is not possible regardless of the direction of rotation without corresponding continuous regeneration. Even with 30 removal cycles, which is equivalent to a process time of 30 min on the used drum filter, the specific solid mass flow rate is reduced by 61 % for TiO₂ and by 13 % for yeast under ideal conditions of this experimental study.
- It is important that the particle-to-pore size ratio is greater than 1.4, so that there is no pore-reducing effect that would decrease the removal efficiency.
- The discharge in the opposite direction is only beneficial if the cohesive forces within the cake are not sufficient to maintain the cake.
- In filtration without gas throughput, the residual moisture is independent of the cake height. Even through free filter surfaces, the residual moisture remains constant.

Cake discharge of thin filter layers by roller discharge is therefore possible, but associated with membrane lifetime challenges.

Data Availability Statement

The data that support the findings of this study are available from the corresponding author upon reasonable request.

Supporting Information

Supporting Information for this article can be found under DOI: <https://doi.org/10.1002/ceat.202300249>.

The authors have declared no conflict of interest.

Acknowledgment

The authors would like to thank the German Federation of Industrial Research Associations (AiF) for the financial support (IGF number 21039 N) and all colleagues and students, especially Simon Egner, for the support in writing this paper. Open access funding enabled and organized by Projekt DEAL.

Symbols used

| | | |
|------------------|---------------------------------------|--------------------------------|
| A | [m ²] | filter surface |
| d | [m] | diameter |
| D | [N m ⁻¹] | spring rate |
| d_{cap} | [m] | diameter of capillary pressure |
| L | [m] | length of the roller |
| M_L | [kg] | liquid mass of the filter cake |
| M_S | [kg] | solid mass of the filter cake |
| \dot{M}_s | [kg h ⁻¹] | solid mass flow |
| \dot{m}_s | [kg m ⁻² h ⁻¹] | specific solid mass flow |

| | | |
|---------------|-----------------------|-----------------------------------|
| m_{sc} | [kg m ⁻²] | specific solid mass per cycle |
| n | [s ⁻¹] | rotational speed |
| P_c | [m ²] | specific filter cake permeability |
| P_{cap} | [Pa] | capillary pressure |
| Q | [-] | completeness of discharge |
| q_p | [N m ⁻¹] | line load of the roller |
| R_C | [m ⁻²] | filter cake resistance |
| R_{FM} | [m ⁻¹] | filter medium resistance |
| RM | [-] | residual moisture |
| s | [m] | spring travel |
| t_{cycle} | [s] | time of cake formation per cycle |
| $V_{E,cycle}$ | [m ³] | filtrate volume per cycle |
| $x_{50, 3}$ | [m] | mass/volume-related modal value |

Greek letters

| | | |
|----------------------|-----------------------|---------------------------------|
| α_H | [m ⁻²] | specific filter cake resistance |
| $\alpha_{Formation}$ | [°] | cake formation angle |
| γ_L | [N m ⁻¹] | surface tension of liquid |
| Δp | [Pa] | pressure difference |
| ε | [-] | porosity |
| κ | [-] | concentration parameter |
| η_L | [Pa s] | dynamic viscosity of the liquid |
| θ | [°] | contact angle of liquid |
| ρ | [kg m ⁻³] | density |

Abbreviations

| | |
|------------------|------------------------------------|
| EPS | extracellular polymeric substances |
| LSM | laser scanning microscopy |
| MFP | mean flow pore |
| PET | polyethylene terephthalate |
| PP | polypropylene |
| TiO ₂ | titanium dioxide |

References

- [1] H. Anlauf, *Wet Cake Filtration*, Wiley-VCH, Weinheim **2019**.
- [2] Y. Chisti, *Biotechnol. Adv.* **2007**, *25* (3), 294–306. DOI: <https://doi.org/10.1016/j.biotechadv.2007.02.001>
- [3] M. Hannon, J. Gimpel, M. Tran, B. Rasala, S. Mayfield, *Biofuels* **2010**, *1* (5), 763–784. DOI: <https://doi.org/10.4155/bfs.10.44>
- [4] E. Molina Grima, E.-H. Belarbi, F. G. Ación Fernández, A. Robles Medina, Y. Chisti, *Biotechnol. Adv.* **2003**, *20* (7–8), 491–515. DOI: [https://doi.org/10.1016/S0734-9750\(02\)00050-2](https://doi.org/10.1016/S0734-9750(02)00050-2)
- [5] J. Hermeler, L. Horstkötter, T. Hartmann, *Filtr. Sep.* **2012**, *26* (3), 158–166.
- [6] K. L. Morrissey et al., *Algal Res.* **2015**, *11*, 304–312. DOI: <https://doi.org/10.1016/j.algal.2015.07.009>
- [7] J. C. Dodd, *Agric. Wastes* **1979**, *1* (1), 23–37. DOI: [https://doi.org/10.1016/0141-4607\(79\)90004-0](https://doi.org/10.1016/0141-4607(79)90004-0)
- [8] J. Bratby, D. Parker, *Proc. Water Environ. Fed.* **2009**, *2009* (7), 7937–7954. DOI: <https://doi.org/10.2175/193864709793900294>
- [9] V. Bächle, P. Morsch, M. Gleiß, H. Nirschl, *Eng.* **2021**, *2* (2), 181–196. DOI: <https://doi.org/10.3390/eng2020012>
- [10] S. Ripperger, J. Altmann, *Sep. Purif. Technol.* **2002**, *26* (1), 19–31. DOI: [https://doi.org/10.1016/S1383-5866\(01\)00113-7](https://doi.org/10.1016/S1383-5866(01)00113-7)
- [11] N. Rossignol, L. Vandanjon, P. Jaouen, F. Quéméneur, *Aquacult. Eng.* **1999**, *20* (3), 191–208. DOI: [https://doi.org/10.1016/S0144-8609\(99\)00018-7](https://doi.org/10.1016/S0144-8609(99)00018-7)
- [12] I. H. Huisman, D. Elzo, E. Middelink, A. Trägårdh, *Colloids Surf.* **1998**, *138* (2–3), 265–281. DOI: [https://doi.org/10.1016/S0927-7757\(96\)03976-3](https://doi.org/10.1016/S0927-7757(96)03976-3)
- [13] R. Bott, T. Langeloh, E. Ehrfeld, *Chem. Eng. J.* **2000**, *80* (1–3), 245–249. DOI: [https://doi.org/10.1016/S1383-5866\(00\)00097-6](https://doi.org/10.1016/S1383-5866(00)00097-6)
- [14] S. S. Lee, A. Burt, G. Russotti, B. Buckland, *Biotechnol. Bioeng.* **1995**, *48* (4), 386–400. DOI: <https://doi.org/10.1002/bit.260480411>
- [15] S. D. Ríos, J. Salvadó, X. Farriol, C. Torras, *Bioresour. Technol.* **2012**, *119*, 406–418. DOI: <https://doi.org/10.1016/j.biortech.2012.05.044>
- [16] H. Anlauf, A. Erk, *Min. Proc.* **2006**, *47*, 22–29.
- [17] A. D. Stickland, R. G. de Kretser, A. R. Kilcullen, P. J. Scales, P. Hillis, M. R. Tillotson, *AIChE J.* **2008**, *54* (2), 464–474. DOI: <https://doi.org/10.1002/aic.11369>
- [18] A. D. Stickland, R. G. de Kretser, P. J. Scales, S. P. Usher, P. Hillis, M. R. Tillotson, *Chem. Eng. Sci.* **2006**, *61* (12), 3818–3829. DOI: <https://doi.org/10.1016/j.ces.2006.01.020>
- [19] K. A. Landman, L. R. White, *AIChE J.* **1997**, *43* (12), 3147–3160. DOI: <https://doi.org/10.1002/aic.690431204>
- [20] E. Ehrfeld, R. Bott, *Filtr. Sep.* **1990**, *27* (4), 274–275. DOI: [https://doi.org/10.1016/0015-1882\(90\)80459-X](https://doi.org/10.1016/0015-1882(90)80459-X)
- [21] Z. Lam, H. Anlauf, H. Nirschl, *Sep. Purif. Technol.* **2019**, *221*, 38–43. DOI: <https://doi.org/10.1016/j.seppur.2019.03.062>
- [22] W. Mores, *J. Membr. Sci.* **2001**, *189* (2), 217–230. DOI: [https://doi.org/10.1016/S0376-7388\(01\)00409-4](https://doi.org/10.1016/S0376-7388(01)00409-4)
- [23] L. Marbelia, M. Mulier, D. Vandamme, K. Muylaert, A. Szymczyk, I. F. Vankelecom, *Algal Res.* **2016**, *19*, 128–137. DOI: <https://doi.org/10.1016/j.algal.2016.08.004>
- [24] Z. Lam, H. Anlauf, H. Nirschl, *Chem. Eng. Technol.* **2021**, *44* (8), 1479–1487. DOI: <https://doi.org/10.1002/ceat.202000615>
- [25] T. Tanaka, S.-I. Tsuneyoshi, W. Kitazawa, K. Nakanishi, *Sep. Sci. Technol.* **1997**, *32* (11), 1885–1898. DOI: <https://doi.org/10.1080/01496399708000743>
- [26] T. Tran, S. Gray, R. Naughton, B. Bolto, *J. Membr. Sci.* **2006**, *280* (1–2), 560–571. DOI: <https://doi.org/10.1016/j.memsci.2006.02.013>
- [27] A. W. Zularisam, A. F. Ismail, R. Salim, *Desalination* **2006**, *194* (1–3), 211–231. DOI: <https://doi.org/10.1016/j.desal.2005.10.030>
- [28] X. Cui, K.-H. Choo, *Environ. Eng. Res.* **2014**, *19* (1), 1–8. DOI: <https://doi.org/10.4491/eer.2014.19.1.001>
- [29] *Handbook of Filter Media*, 2nd ed. (Eds: D. Purchas, K. Sutherland), Elsevier Advanced Technology, Oxford **2002**.